

# Bridging the Last Mile in Sim-to-Real Robot Perception via Bayesian Active Learning

Jianxiang Feng<sup>1,2</sup>, Jongseok Lee<sup>1</sup>, Maximilian Durner<sup>1,2</sup> and Rudolph Triebel<sup>1,2</sup>

**Abstract**—Learning from synthetic data is popular in a variety of robotic vision tasks such as object detection, because large amount of data can be generated without annotations by humans. However, when relying only on synthetic data, we encounter the well-known problem of the simulation-to-reality (Sim-to-Real) gap, which is hard to resolve completely in practice. For such cases, real human-annotated data is necessary to bridge this gap, and in our work we focus on how to acquire this data efficiently. Therefore, we propose a Sim-to-Real pipeline that relies on deep Bayesian active learning and aims to minimize the manual annotation efforts. We devise a learning paradigm that autonomously selects the data that is considered useful for the human expert to annotate. To achieve this, a Bayesian Neural Network (BNN) object detector providing reliable uncertain estimates is adapted to infer the informativeness of the unlabeled data, in order to perform active learning. In our experiments on two object detection data sets, we show that the labeling effort required to bridge the reality gap can be reduced to a small amount. Furthermore, we demonstrate the practical effectiveness of this idea in a grasping task on an assistive robot.

## I. INTRODUCTION

Over the last years, the performance of computer vision increased sharply, leading to the urge of employing such approaches on robotic vision tasks such as object detection [1], pose estimation [2] and vision guided grasping [3]. In this context, a main issue is necessity of large amounts of annotated, task-related training data. Therefore, a compelling solution is to learn from synthetic data. Like this, large amount of annotated data can be obtained from simulation with relatively less time and manual efforts [3]–[5]. With the emergence of open-source image synthesizing pipelines like [6]–[9], this solution becomes even more accessible in practice. However, although these pipelines continue improving in fidelity and become more photorealistic, there are subtle but important differences between simulation and reality. This leads to the so-called *reality gap* which is the main barrier of transferring simulated knowledge on real world robotic perception. Previous works address this gap by applying techniques such as Domain Randomization (DR) [5], [10] and Domain Adaptation (DA) [3], [11] with certain improvements. Yet, the unpredictable variability of real-world scenes prevent a complete elimination of the reality gap [12].

The same issue we faced on our robotic platform EDAN [13], where we have used photorealistic synthetic

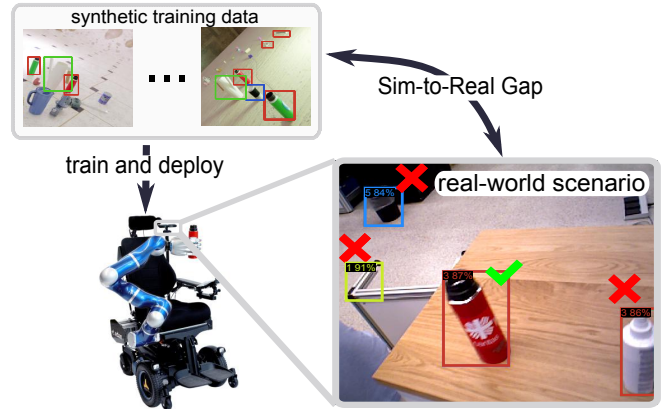


Fig. 1. Illustration of a practical problem. Deploying a detector trained with only synthetic images on real-world scenarios leads to under-performances. These inaccuracies (denoted by red crosses) such as false positives are due to the Sim-to-Real gap and for this, a few informative real images can improve the performance. Therefore, this work investigates the question on how to collect such informative real images via active learning.

images to train an object detector [1]. However, from our experience, the variables such as sensor characteristics, illuminations and textures cannot be modeled to precisely match the real environments. Even after a careful tuning of DR, we find that the object detector fails to generalize well in our real-world scenario. To overcome this, we applied task-oriented fine-tuning, by using real data of the underlying robotic application, like [14]–[16]. Hence, based on our use-case, we advocate that real data is indispensable for a robot to adapt from simulation to real world.

This however, comes with the requirement of tedious, time consuming manual labeling. Thus, in this work, we investigate on the question: *How to collect real data with minimum annotation efforts?* Having an object detector trained on synthetic images, we propose an active learning pipeline that bridges the last mile of the reality gap with few annotated real images. Based on a deep Bayesian active learning framework, we analyze different strategies to automatically select the most informative data samples for the detector. The basic idea is, by enabling the detector itself to choose important, uncertain images we can reduce the amount of data samples which have to be annotated (see Fig. 2).

More concretely, we train a BNN for object detection with photorealistic synthetic images, generated by Blender-Proc [8], a physically based rendering image synthesizer, along with domain randomization. In the second step, task-related real images are forwarded to the detector, which ranks the images based on an information theoretic acquisition function. To reduce the labeling effort, a subset of the

<sup>1</sup> Institute of Robotics and Mechatronics, German Aerospace Center (DLR), Wessling, Germany. email: jianxiang.feng@dlr.de

<sup>2</sup> Department of Computer Science, Technical University of Munich (TUM), Garching, Germany.

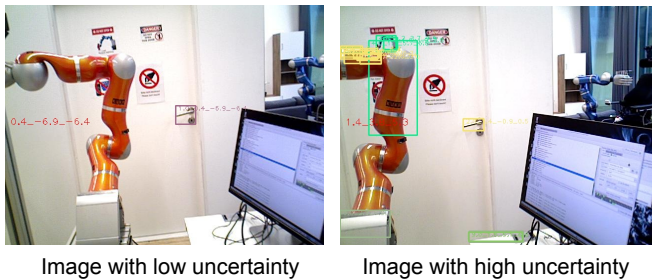


Fig. 2. **An illustrative example.** The images show detection results of a detector trained on door handles. While for humans, no evident variance exists for the above figures, the detection results show a significant difference in terms of uncertainty scores or informativeness. Active learning motivates that the sample with high uncertainty score is more informative for the object detector to increase its performance than the lower one.

samples according to a sampling strategy is selected and a human expert is asked to annotate them. The annotated data is then used to fine-tune the model and bridge the reality gap. This step can be repeated iteratively until this gap is eliminated completely. Besides the empiric validation of the proposed idea on two data sets, we deploy the pipeline on our real robot and show a significant positive impact of the visual perception within the grasping tasks.

In summary, the main contributions of this work are:

- we propose to bridge the reality gap by applying a BNN in an active learning framework for object detection.
- we identify the foreground class imbalance problem as detrimental within our pipeline and examine several sampling strategies to address it in practice.
- we conduct experiments to empirically show the positive impact of the proposed pipeline on two data sets which enables a reduction of samples to be labeled up to  $\sim 60\%$ . Furthermore, we demonstrate its applicability in reducing labeling efforts on a real robotic system.

Importantly, the accompanying video provides qualitative results including the demonstration on an assistive robot.

## II. RELATED WORK

*a) Bridging Sim-to-Real Gap:* Sim-to-Real transfer is mainly tackled with DR and DA. The former treats the real test scenario as one instance of many synthetic ones generated by randomizing the parameters of the synthesizer such as materials, lightening, backgrounds, and plausible geometric configurations. Related examples can be seen in [5], [10], [17], [18]. In contrast, DA focuses on learning domain-invariant representations across the different domains (here: synthetic and real domain) by sometimes including data of the target domain, e.g., the previous works of [3], [11], [16], [19]–[21]. Besides these two techniques, the paradigm of active learning is appealing to address the reality gap by utilizing annotated real data in an efficient way. In pool-set based active learning [22], the aim is to reach certain level of performance with as less data as possible. For supervised learning, the data is selected based on their informativeness, which can be measured by different quantities such as the output uncertainty, the disagreement of a committee, or the expected model change [23], [24]. We also stress

that active learning is complementary to the aforementioned techniques. While some works [25], [26] argue for the fusion of DA and active learning to obtain better performance, we additionally use DR in this work. Su *et al.* [25] combine the adversarial learning and importance sampling for active domain adaptation. Zhou *et al.* [26] propose a three-stage active adversarial learning neural network for this purpose. Nevertheless, none of them considers employing BNNs for this purpose. Wen *et al.* [27] apply BNNs for DA, but they only focus on conventional passive learning paradigm and classification tasks. We aim to study the active learning paradigm for Sim-to-Real on a challenging real-world object detection task, which is arguably more relevant for various use-cases of the robots.

*b) Active Learning for Object Detection:* In the context of active learning for object detection, specific metrics related to characteristics of the underlying network can be applied [28]. While in [29] the margin of the bounding box scores in different layers is used, Kao *et al.* [30] consider the localization tightness and stability. Yoo and Kweon [31] propose to learn a specific active learning loss with an additional head. Meanwhile, uncertainty based approaches [23], [32] are also able to achieve competitive performances in the field of object detection. Most of uncertainty based approaches are built on BNNs [33], [34] which can produce more reliable uncertainty estimates. Along with its theoretic soundness, the task-agnostic characteristic of these approaches can facilitate wider applicability for different domains. Most of previous work integrate BNNs into the detection head of current object detectors [35]. While some only exploit the classification branch for the uncertainty estimation [36], others [37], [38] consider both classification and regression branches. Yet, they rely on larger amount of annotated real world data to initialize the training of the model and update the model in each iteration, while we assume relatively few real data.

## III. PROBLEM FORMULATION AND OVERVIEW

To formulate the problem, we consider two domains namely the simulation domain  $S$  and the real/target domain  $R$ . In the simulation domain  $S$ , we assume the availability of annotated data set, i.e., given the synthetic data  $\mathbf{x}^S$  and annotated labels  $\mathbf{y}^S$ , we denote the synthetic data set as  $\mathcal{D}_S = \{(\mathbf{x}_i^S, \mathbf{y}_i^S)\}_{i=1}^{N_S}$  where  $N_S$  is the number of data points. In contrary, the real domain  $R$  contains an unlabeled data set  $\mathcal{D}_T = \{(\mathbf{x}_i^R)\}_{i=1}^{N_R}$  which constitutes of  $N_R$  number of real images  $\mathbf{x}^R$ . Considering the object detection tasks, a supervised learning problem is assumed to train an object detector. Concretely, given the space of inputs  $\mathcal{X}$  (both synthetic and real images) and outputs  $\mathcal{Y}$  (sets of object classes  $\mathbf{c}$  and their 2D location as bounding boxes  $\mathbf{b}$ ), we define the object detector as a function  $\mathcal{M}_\theta : \mathcal{X} \rightarrow \mathcal{Y}$  with the weights  $\theta$ . Naturally, our objective is to obtain an object detector in the real domain  $R$ , for which synthetic data  $\mathcal{D}_S$  can be exploited.

To achieve this goal, the proposed pipeline (depicted in Fig. 3) relies on deep Bayesian active learning. The motivation of our approach is that in practice, this so-called Sim-

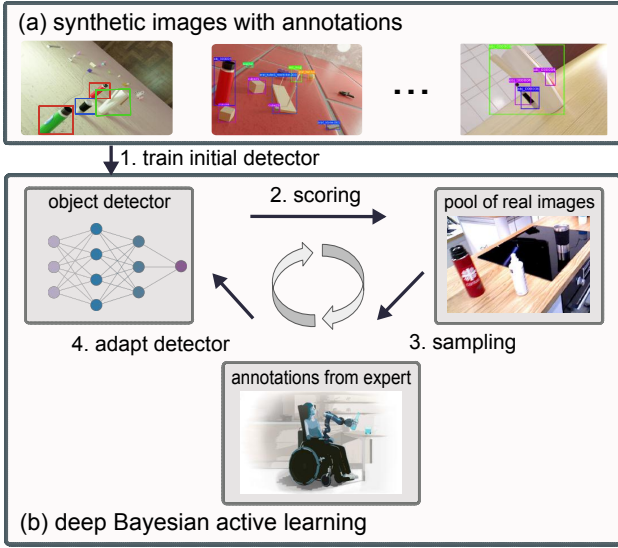


Fig. 3. **The proposed Sim-to-Real pipeline.** Using labeled synthetic images, we first train an initial BNN object detector. Then, we rely on deep Bayesian active learning to select the most informative images from a pool of unlabeled real images. The scoring of all the images in the pool is achieved via an acquisition function, while sampling is applied to deal with the foreground class imbalance problem. Based on the selected images, the human expert performs the annotation and the detector is adapted via fine-tuning. The process is repeated until the reality gap is bridged.

to-Real transfer can be achieved by combining (a) the large amounts of annotated synthetic data, and (b) a few but the most informative real images with annotations from human expert. Importantly, we conjecture that the real images can bridge the reality gap in a simple and effective manner, and thus, this work focuses on reducing the amounts of needed real images. For this, as shown in Fig. 3, (i) we use  $\mathcal{D}_S$  to train an initial model with domain randomization. (ii) Then, treating the unlabeled real data  $\mathcal{D}_T$  as a pool set  $\mathcal{D}_{pool}$ , we rank the informativeness of each images with an acquisition function  $\mathcal{A}(\cdot)$  and then (iii) apply a sampling strategy to create a subset. (iv) The labels of this subset is queried to a human expert for manual annotation. This process can be repeated for multiple times until the reality gap is diminished. Next, we describe and motivate these steps in detail.

#### IV. THE PROPOSED PIPELINE

This section describes our pipeline for Sim-to-Real transfer for 2D object detection. The main components are a BNN object detector for uncertainty quantification (Sec. IV-A), and deep Bayesian active learning framework (Sec. IV-B).

##### A. Bayesian Neural Networks for Object Detection

We choose to model the object detector  $\mathcal{M}_\theta$  as a BNN, in order to obtain its uncertainty estimates. BNNs achieve this by reasoning about the model uncertainty, which indicates *what the model does not know*. Reasoning about the model uncertainty, the active learning framework can later leverage this information to label the most uncertainty data to the model itself. To do so, given the training data  $\mathcal{D}_{train}$  and a test data sample  $\mathbf{x}^*$ , BNNs produce the output distribution  $p(\mathbf{y}^* |$

$\mathbf{x}^*, \mathcal{D}_{train})$  by marginalizing over the models' distribution:

$$p(\mathbf{y}^* | \mathbf{x}^*, \mathcal{D}_{train}) = \int p(\mathbf{y}^* | \mathbf{x}^*, \theta) p(\theta | \mathcal{D}_{train}) d\theta. \quad (1)$$

In (1),  $p(\mathbf{y}^* | \mathbf{x}^*, \theta)$  is the observation likelihood, and  $p(\theta | \mathcal{D}_{train})$  is the distribution over the weights  $\theta$ . As a closed form solution to the integral in (1) does not exist, the Monte-Carlo integration is often used for a numerically solution [39]. As a note, our active learning pipeline uses both the synthetic and the annotated real images as the training set  $\mathcal{D}_{train}$ , and the new images  $\mathbf{x}^*$  are samples from the pool set  $\mathcal{D}_{pool}$ .

However, applying BNNs to the existing anchor-based detectors such as Retinanet [1] requires several adaptations [36], [38]. This is due to their post-processing steps, e.g., (i) *miss-correspondence between the anchor predictions and final outputs*, and (ii) *hard cut-off behavior in non-maximum suppression (NMS) step*. For these, the BayesOD framework [38] can be used, which performs Monte-Carlo sampling for each anchor prediction before NMS steps, and relies on Bayesian inference to infer the output distributions. Intuitively, BayesOD clusters outputs in anchor level using spatial affinity. To explain, assume that such cluster contains  $M$  anchors and consider the highest classification score as center of this cluster (indexed by 1). The other outputs are considered as measurements to provide information for the center, denoted by  $\hat{\mathbf{c}}_1$  and  $\hat{\mathbf{b}}_1$ . By further denoting the final predictive distributions for classification and regression of this cluster as  $p_{[\hat{\mathbf{c}}_1, \dots, \hat{\mathbf{c}}_M]}(\mathbf{c} | \mathbf{x}^*, \mathcal{D}_{train})$  and as  $p_{[\hat{\mathbf{b}}_1, \dots, \hat{\mathbf{b}}_M]}(\mathbf{b} | \mathbf{x}^*, \mathcal{D}_{train})$  respectively, the final output distributions are computed as:

$$p_{[\hat{\mathbf{c}}_1, \dots, \hat{\mathbf{c}}_M]}(\mathbf{c} | \mathbf{x}^*, \mathcal{D}_{train}) \propto p_{\hat{\mathbf{c}}_1}(\mathbf{c} | \mathbf{x}^*, \mathcal{D}_{train}) \prod_{i=2}^m p(\hat{\mathbf{c}}_i | \mathbf{c}, \mathbf{x}^*, \mathcal{D}_{train}), \quad (2)$$

$$p_{[\hat{\mathbf{b}}_1, \dots, \hat{\mathbf{b}}_M]}(\mathbf{b} | \mathbf{x}^*, \mathcal{D}_{train}) \propto p_{\hat{\mathbf{b}}_1}(\mathbf{b} | \mathbf{x}^*, \mathcal{D}_{train}) \prod_{i=2}^m p(\hat{\mathbf{b}}_i | \mathbf{b}, \mathbf{x}^*, \mathcal{D}_{train}). \quad (3)$$

Here,  $p_{\hat{\mathbf{c}}_1}(\mathbf{c} | \mathbf{x}^*, \mathcal{D}_{train})$  represents the per-anchor predictive distribution of the cluster center, while  $\prod_{i=2}^m p(\hat{\mathbf{b}}_i | \mathbf{b}, \mathbf{x}^*, \mathcal{D}_{train})$  is the likelihood of each cluster member given the output. When we choose the Gaussian and Categorical distributions for regression and classification tasks respectively, the sufficient statistics of them such as mean and covariance matrix can be computed analytically. We refer more details in [38] and next, we discuss the active learning framework that relies on the BayesOD framework.

##### B. Bayesian Active Learning for Sim-to-Real

With the uncertainty estimates of an object detector, the active learning pipeline needs to choose the images for annotation. This selection of images is done via an acquisition function. Moreover, due to the foreground class imbalance, sampling strategy also needs to be devised. We describe below these components and our design choices.

1) *Acquisition Function:* For deep Bayesian active learning, we define the acquisition function based on the uncertainty estimates from the BNN detector. In this step, the acquisition function is used to obtain the informativeness

scores for each detected instance on one image, and then *aggregated* into one final score to represent the informativeness of the entire image. Once the scores are obtained for all the images in the pool set  $\mathcal{D}_{pool}$ , we sample a subset of them for annotation (IV-B.2) in order to retrain the model. We repeat this step iteratively for reaching a certain level of performance. Specifically, we consider uncertainty from both category classification and bounding box regression, which are referred to as semantic and spatial uncertainty respectively [40]. To this end, we define the semantic uncertainty for the  $j$ -th detection instance on an image, as the sum of entropy of each output dimension. So, given the Shannon Entropy measure  $\mathcal{H}(\cdot)$  [41], the classification acquisition function  $\mathcal{U}_{j,cls}$  is modeled with a Bernoulli distribution as:

$$\begin{aligned} \mathcal{U}_{j,cls} &= \sum_{i=1}^{|\mathcal{C}|} \mathcal{H}(p(c_i|\mathbf{x}^*, \mathcal{D}_{train})), \\ &= \sum_{i=1}^{|\mathcal{C}|} [-p(c_i|\mathbf{x}^*, \mathcal{D}_{train}) \log p(c_i|\mathbf{x}^*, \mathcal{D}_{train}) \\ &\quad - (1 - p(c_i|\mathbf{x}^*, \mathcal{D}_{train})) \log (1 - p(c_i|\mathbf{x}^*, \mathcal{D}_{train}))]. \end{aligned} \quad (4)$$

In (4), the steps follows from the definition of the entropy, and optimizing the given measure is equivalent to maximizing the information gain [42] or information content.

The uncertainty from regression is defined as the differential entropy of  $p(\mathbf{b}|\mathbf{x}^*, \mathcal{D}_{train})$  which is approximated by a multivariate Gaussian with mean  $\hat{\mathbf{b}}$  and covariance matrix  $\mathbf{C}_b$  calculated from the samples of predicted bounding boxes:

$$\begin{aligned} \mathcal{U}_{j,reg} &= \mathcal{H}(p(\mathbf{b}|\mathbf{x}^*, \mathcal{D}_{train})) \\ &= \frac{k}{2} + \frac{k}{2} \ln(2\pi) + \frac{1}{2} \ln(|\mathbf{C}_b|), \end{aligned} \quad (5)$$

where  $k$  is the dimensionality of the random variable  $\mathbf{b}$ . Again, this regression acquisition function  $\mathcal{U}_{j,reg}$  follows from the definition of entropy for Gaussian distributions, and represents the information content of an image.

We choose to exploit these two quantities by a combination function  $comb(\cdot)$ , in order to produce the uncertainty score for each of  $N_k$  detected instance on  $k$ -th image. Then, the acquisition function for  $k$ -th image  $\mathcal{A}$  is defined by aggregating scores with a function  $agg(\cdot)$  denoted by:

$$\mathcal{A}(\mathbf{x}_k) = agg_{j \in N_k}(comb(\mathcal{U}_{j,cls}, \mathcal{U}_{j,reg})), \quad (6)$$

The combination function  $comb(\cdot)$  can be a weighted sum or max operation [32]. The aggregation function  $agg(\cdot)$  can be a sum or average operation [29]. What motivates such combinations is the problem itself, i.e. object detection involves both the classification and the regression tasks.

2) *Sampling Strategy*: A naive strategy is to rank the images with an acquisition function and then take top  $B$  ones, which represents the most informative data points. However, this strategy assumes that the foreground classes are well balanced [43], [44]. Thus, when the foreground classes are imbalanced in practice, the performance gain from active learning can degrade [43], [44]. In order to conquer this, we employ a geometry-based sampling method called core-set [45] and also introduce a simpler alternative below.

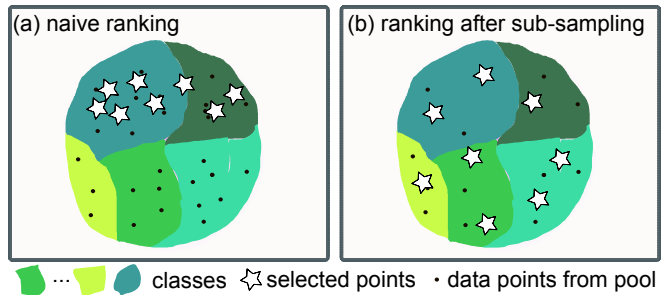


Fig. 4. **Sub-sampling Strategy.** We illustrate the ranking after sub-sampling strategy. A naive ranking selects the most informative points from a few classes of pool data, while the ranking after sub-sampling enables to evenly select the most informative points across the variety of classes. This mitigates the foreground class imbalance problem of active learning for object detection, and introduced diversity can improve the performance.

a) *Core-set*: The core-set approach aims to select most representative subset by increasing the variations of data from the pool set. This is achieved by minimizing a core-set loss which upper bounds the generalization loss in active learning [45]. Its greedy version can be implemented as a  $k$ -center algorithm, which selects  $B$  points in the pool set, that have the largest distance with their nearest neighbors in the previously selected data set. Specifically, we devise the distance function  $\Delta(\mathbf{x}_i, \mathbf{x}_j)_{\mathbf{x}_i \in \mathcal{D}_{pool}, \mathbf{x}_j \in \mathbf{s}_0}$  for selecting the nearest neighbor based on uncertainty estimates:

$$\Delta(\mathbf{x}_i, \mathbf{x}_j)_{\mathbf{x}_i \in \mathcal{D}_{pool}, \mathbf{x}_j \in \mathbf{s}_0} = \left\| \sum_{k=1}^{N_i} p(\mathbf{c}_k|\mathbf{x}_i) - \sum_{k=1}^{N_j} p(\mathbf{c}_k|\mathbf{x}_j) \right\|_2 + w \mathcal{A}(\mathbf{x}_i) \quad (7)$$

where  $w$  is a weight for the uncertainty term and  $\mathbf{s}_0$  is the set of previously selected data points, which can be initialized randomly at the first step.

b) *Ranking after sub-sampling*: We further devise a simpler alternative. Our intuition is that the uniformly random selection can lead to more balanced foreground class distribution. By assuming there is certain degree of redundancy in the data set, we rank the most uncertain examples after sub-sampling uniformly. With this, the pool of the choices can be balanced first, and the acquisition function can thus choose by taking into account the variations in the selected data. The idea is illustrated in Fig. 4.

## V. EXPERIMENT

In this section, we validate and evaluate the proposed idea on a self-collected daily objects data set — the EDAN data set, the YCBV [46], [47] public data set, and a grasping task on an assistive robot. We stress that the self-collected data set originates from a robotic vision-based shared control grasping task [48], which is executed in a real environment with more relevance to our scenario than the YCBV dataset. The implementation details and parameter settings of the proposed pipeline are then provided, which is followed by our results and discussions.

a) *Datasets*: (1) The EDAN data set includes five objects which are ikea bottle, watering can, door handle, drawer handle and grey mug. The real image data set with  $\sim 1.5k$  images captured, annotated manually and split into



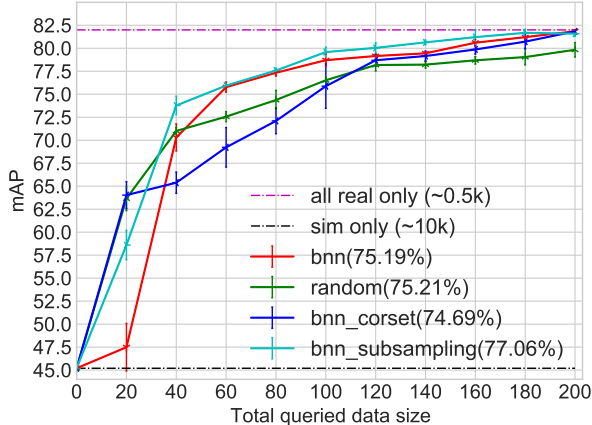


Fig. 6. **Results on the EDAN data set.** Active learning result plots with standard deviation for 3 random runs on the EDAN data set ( with 10 iterations and 20 images queried in each iteration). Values in the parentheses are mean mAP over 10 iterations.

tions in Fig. 6. In the figure, we can see that the BNN detector with sub-sampling strategy (“bnn\_subsampling”) performs the best on this data set, outperforming the random baseline for around  $\sim 2$  mAP averagely over 10 iterations. Moreover, BNNs with core-set approach (“bnn\_coreset”) underperforms at the beginning, but is able to achieve higher mAP than “random” in later iterations. More importantly, the BNN with sub-sampling approach can reach the performance of the model trained only on the real data set by **saving around 60% annotation efforts**, thus bridging the reality gap.

	Random selection	Naive ranking	Sub-sampling	Core-set
EDAN	360	872	853	<b>635</b>
YCBV	5623	8817	8453	<b>6410</b>

TABLE II

INTER CLASS VARIATIONS FOR THE SELECTED DATA SET IN EACH ITERATION DURING ACTIVE LEARNING. LOWER THE BETTER.

c) *Results on the YCBV data set:* The results on the YCBV data set is shown in Fig 7. We can see that the reality gap can be bridged mostly by just one third of all data in the pool set. Though the random selection can provide competitive performance averagely across 10 iterations, similar to the results reported by a previous work [24], the BNN detector with core-set approach (“bnn\_coreset”) is able to bridge the gap faster in the later iterations. However, on the YCBV data set, the performance plateaus in the regimes with more than 50 data points (also observed in [24]). We attribute the performance plateau to the larger inter class variations than the EDAN data set. As evidenced in Tab. II, the total variations across all the strategies are higher in the YCBV data set. We find that the large inter class variations can have a negative impact on the active learning process in practice. On the other hand, when the inter class variations are relatively small (e.g. the EDAN data set), our proposed pipeline demonstrates that the Sim-to-Real gap can be bridged with high real data efficiency.

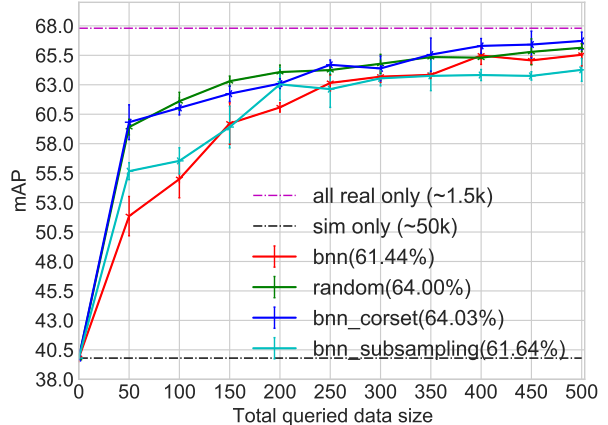


Fig. 7. **Results on the YCBV data set.** Active learning result plots with standard deviation for 3 random runs on the YCBV data set ( with 10 iterations and 50 images queried in each iteration). Values in the parentheses are mean mAP over 10 iterations.

## B. Deployment on EDAN

An accurate object detector is demonstrated for diverse tasks on the assistive robotic platform, EDAN [13], e.g., door opening [52] and watering pouring [48], [53]. Due to the use-cases of an assistive robot, a variety of objects need to be detected in different environments, and the manual efforts required for adaptation must be kept as minimum as possible. Therefore, we show the effectiveness of proposed idea in a shared control grasping task on EDAN, where a user (e.g. people with motor disability) sitting on the chair intends to control the robot arm by using an interface (EMG signal [54] or spacemouse), which has lower degrees of freedom than that of the end effector (3 vs. 6), to achieve the considered tasks. To precisely detect and localize the object is thus a prerequisite for the shared control method [48], which can ease the execution of the task for the user with the given interface. Besides the adapted detector, we employ the Augmented autoencoder (AAE) and Iterative Closest Point (ICP) pipeline in [2] for accurate pose estimation. We provide a video to showcase the deployment.

## VI. CONCLUSIONS

This paper presents a Sim-to-Real pipeline, in which, an object detector is initially trained with synthetic data. Then, observing the sub-optimal performance of learning from only simulation, we propose to efficiently use real annotated data via exploiting deep Bayesian active learning. Empirically, we demonstrate the encouraging impact of the proposed pipeline on two data sets, and further show its applicability on a real robotic system. In particular, our experiments indicate that the foreground class imbalance can be one of the factors which can determine the success of our pipeline in practice. More importantly, our work provides an empirical evidence that the real annotated images can efficiently reduce the reality gap in practice — the proposed pipeline can enable a reduction upto 60% of the amounts of real annotated images that are needed to diminish this real gap.

## REFERENCES

- [1] T.-Y. Lin, P. Goyal, R. Girshick, K. He, and P. Dollár, “Focal loss for dense object detection,” in *Proceedings of the IEEE international conference on computer vision*, 2017, pp. 2980–2988.
- [2] M. Sundermeyer, Z.-C. Marton, M. Durner, and R. Triebel, “Augmented autoencoders: Implicit 3d orientation learning for 6d object detection,” *International Journal of Computer Vision*, vol. 128, no. 3, pp. 714–729, 2020.
- [3] K. Bousmalis, A. Irpan, P. Wohlhart, Y. Bai, M. Kelcey, M. Kalakrishnan, L. Downs, J. Ibarz, P. Pastor, K. Konolige *et al.*, “Using simulation and domain adaptation to improve efficiency of deep robotic grasping,” in *2018 IEEE international conference on robotics and automation (ICRA)*. IEEE, 2018, pp. 4243–4250.
- [4] G. Georgakis, A. Mousavian, A. C. Berg, and J. Kosecka, “Synthesizing training data for object detection in indoor scenes,” *arXiv preprint arXiv:1702.07836*, 2017.
- [5] J. Tobin, R. Fong, A. Ray, J. Schneider, W. Zaremba, and P. Abbeel, “Domain Randomization for Transferring Deep Neural Networks from Simulation to the Real World,” *2017 IEEE/RSJ International Conference on Intelligent Robots and Systems (IROS)*, pp. 23–30, 2017.
- [6] A. Dosovitskiy, G. Ros, F. Codevilla, A. Lopez, and V. Koltun, “CARLA: An open urban driving simulator,” in *1st Annual Conference on Robot Learning*, 2017.
- [7] T. To, J. Tremblay, D. McKay, Y. Yamaguchi, K. Leung, A. Balanon, J. Cheng, W. Hodge, and S. Birchfield, “NDDS: NVIDIA deep learning dataset synthesizer,” 2018.
- [8] M. Denninger, M. Sundermeyer, D. Winkelbauer, Y. Zidan, D. Olefir, M. Elbadrawy, A. Lodhi, and H. Katam, “Blenderproc,” *arXiv preprint arXiv:1911.01911*, 2019.
- [9] M. G. Müller, M. Durner, A. Gawel, W. Stürzl, R. Triebel, and R. Siegwart, “A Photorealistic Terrain Simulation Pipeline for Unstructured Outdoor Environments,” in *IEEE/RSJ International Conference on Intelligent Robots and Systems*, 2021.
- [10] R. Alghonaim and E. Johns, “Benchmarking Domain Randomisation for Visual Sim-to-Real Transfer,” *arXiv*, 2020.
- [11] A. K. Tanwani, “Domain invariant representation learning for sim-to-real transfer,” in *Proceedings of the 4th Conference on Robot Learning*, 2020.
- [12] M. Ranaweera and Q. H. Mahmoud, “Virtual to real-world transfer learning: A systematic review,” *Electronics*, vol. 10, no. 12, 2021. [Online]. Available: <https://www.mdpi.com/2079-9292/10/12/1491>
- [13] J. Vogel, A. Hagenhuber, M. Iskandar, G. Quere, U. Leipscher, S. Bustamante, A. Dietrich, H. Höppner, D. Leidner, and A. Albuschäffer, “Edan: An emg-controlled daily assistant to help people with physical disabilities,” in *2020 IEEE/RSJ International Conference on Intelligent Robots and Systems (IROS)*. IEEE, 2020, pp. 4183–4190.
- [14] M. Durner, S. Kriegel, S. Riedel, M. Brucker, Z. Márton, F. Bálint-Benczédi, and R. Triebel, “Experience-based optimization of robotic perception,” in *2017 18th International Conference on Advanced Robotics (ICAR)*, Jul. 2017, pp. 32–39.
- [15] F. Bálint-Benczédi, Z.-C. Márton, M. Durner, and M. Beetz, “Storing and retrieving perceptual episodic memories for long-term manipulation tasks,” in *2017 18th International Conference on Advanced Robotics (ICAR)*, 2017, pp. 25–31.
- [16] X. Zhu, J. Pang, C. Yang, J. Shi, and D. Lin, “Adapting object detectors via selective cross-domain alignment,” in *Proceedings of the IEEE/CVF Conference on Computer Vision and Pattern Recognition*, 2019, pp. 687–696.
- [17] S. Hinterstoisser, V. Lepetit, P. Wohlhart, and K. Konolige, “On pre-trained image features and synthetic images for deep learning,” in *Proceedings of the European Conference on Computer Vision (ECCV) Workshops*, 2018, pp. 0–0.
- [18] T. Hodan, V. Vineet, R. Gal, E. Shalev, J. Hanzelka, T. Connell, P. Urbina, S. N. Sinha, and B. Guenter, “Photorealistic Image Synthesis for Object Instance Detection,” *arXiv*, 2019.
- [19] Y. Chen, W. Li, C. Sakaridis, D. Dai, and L. Van Gool, “Domain adaptive faster r-cnn for object detection in the wild,” in *Proceedings of the IEEE conference on computer vision and pattern recognition*, 2018, pp. 3339–3348.
- [20] N. Inoue, R. Furuta, T. Yamasaki, and K. Aizawa, “Cross-domain weakly-supervised object detection through progressive domain adaptation,” in *Proceedings of the IEEE conference on computer vision and pattern recognition*, 2018, pp. 5001–5009.
- [21] A. Raj, V. P. Namboodiri, and T. Tuytelaars, “Subspace alignment based domain adaptation for rcnn detector,” *arXiv preprint arXiv:1507.05578*, 2015.
- [22] D. A. Cohn, Z. Ghahramani, and M. I. Jordan, “Active learning with statistical models,” *Journal of artificial intelligence research*, vol. 4, pp. 129–145, 1996.
- [23] D. Feng, X. Wei, L. Rosenbaum, A. Maki, and K. Dietmayer, “Deep active learning for efficient training of a lidar 3d object detector,” in *2019 IEEE Intelligent Vehicles Symposium (IV)*. IEEE, 2019, pp. 667–674.
- [24] A. Kirsch, J. Van Amersfoort, and Y. Gal, “Batchbald: Efficient and diverse batch acquisition for deep bayesian active learning,” *Advances in neural information processing systems*, vol. 32, pp. 7026–7037, 2019.
- [25] J.-C. Su, Y.-H. Tsai, K. Sohn, B. Liu, S. Maji, and M. Chandraker, “Active adversarial domain adaptation,” in *Proceedings of the IEEE/CVF Winter Conference on Applications of Computer Vision*, 2020, pp. 739–748.
- [26] F. Zhou, C. Shui, S. Yang, B. Huang, B. Wang, and B. Chaib-draa, “Discriminative active learning for domain adaptation,” *Knowledge-Based Systems*, vol. 222, p. 106986, 2021.
- [27] J. Wen, N. Zheng, J. Yuan, Z. Gong, and C. Chen, “Bayesian uncertainty matching for unsupervised domain adaptation,” *arXiv preprint arXiv:1906.09693*, 2019.
- [28] H. H. Aghdam, A. Gonzalez-Garcia, J. v. d. Weijer, and A. M. López, “Active learning for deep detection neural networks,” in *Proceedings of the IEEE/CVF International Conference on Computer Vision*, 2019, pp. 3672–3680.
- [29] S. Roy, A. Unmesh, and V. P. Namboodiri, “Deep active learning for object detection,” in *BMVC*, vol. 362, 2018, p. 91.
- [30] C.-C. Kao, T.-Y. Lee, P. Sen, and M.-Y. Liu, “Localization-aware active learning for object detection,” in *Asian Conference on Computer Vision*. Springer, 2018, pp. 506–522.
- [31] D. Yoo and I. S. Kweon, “Learning loss for active learning,” in *Proceedings of the IEEE/CVF Conference on Computer Vision and Pattern Recognition*, 2019, pp. 93–102.
- [32] J. Choi, I. Elezi, H.-J. Lee, C. Farabet, and J. M. Alvarez, “Active learning for deep object detection via probabilistic modeling,” *arXiv preprint arXiv:2103.16130*, 2021.
- [33] Y. Gal and Z. Ghahramani, “Dropout as a bayesian approximation: Representing model uncertainty in deep learning,” in *international conference on machine learning*. PMLR, 2016, pp. 1050–1059.
- [34] J. Lee, M. Humt, J. Feng, and R. Triebel, “Estimating model uncertainty of neural networks in sparse information form,” in *International Conference on Machine Learning*. PMLR, 2020, pp. 5702–5713.
- [35] D. Feng, A. Harakeh, S. Waslander, and K. Dietmayer, “A review and comparative study on probabilistic object detection in autonomous driving,” *arXiv preprint arXiv:2011.10671*, 2020.
- [36] D. Miller, L. Nicholson, F. Dayoub, and N. Stünderhauf, “Dropout sampling for robust object detection in open-set conditions,” in *2018 IEEE International Conference on Robotics and Automation (ICRA)*. IEEE, 2018, pp. 3243–3249.
- [37] D. Feng, L. Rosenbaum, and K. Dietmayer, “Towards safe autonomous driving: Capture uncertainty in the deep neural network for lidar 3d vehicle detection,” in *2018 21st International Conference on Intelligent Transportation Systems (ITSC)*. IEEE, 2018, pp. 3266–3273.
- [38] A. Harakeh, M. Smart, and S. L. Waslander, “Bayesod: A bayesian approach for uncertainty estimation in deep object detectors,” in *2020 IEEE International Conference on Robotics and Automation (ICRA)*. IEEE, 2020, pp. 87–93.
- [39] J. Gawlikowski, C. R. N. Tassi, M. Ali, J. Lee, M. Humt, J. Feng, A. Kruspe, R. Triebel, P. Jung, R. Roscher *et al.*, “A survey of uncertainty in deep neural networks,” *arXiv preprint arXiv:2107.03342*, 2021.
- [40] D. Hall, F. Dayoub, J. Skinner, H. Zhang, D. Miller, P. Corke, G. Carneiro, A. Angelova, and N. Stünderhauf, “Probabilistic object detection: Definition and evaluation,” in *Proceedings of the IEEE/CVF Winter Conference on Applications of Computer Vision*, 2020, pp. 1031–1040.
- [41] C. E. Shannon, “A mathematical theory of communication,” *ACM SIGMOBILE mobile computing and communications review*, vol. 5, no. 1, pp. 3–55, 2001.
- [42] D. J. MacKay, “Information-based objective functions for active data selection,” *Neural computation*, vol. 4, no. 4, pp. 590–604, 1992.

- [43] U. Aggarwal, A. Popescu, and C. Hudelot, "Active learning for imbalanced datasets," in *Proceedings of the IEEE/CVF Winter Conference on Applications of Computer Vision*, 2020, pp. 1428–1437.
- [44] K. Oksuz, B. C. Cam, S. Kalkan, and E. Akbas, "Imbalance problems in object detection: A review," *IEEE transactions on pattern analysis and machine intelligence*, 2020.
- [45] O. Sener and S. Savarese, "Active learning for convolutional neural networks: A core-set approach," *arXiv preprint arXiv:1708.00489*, 2017.
- [46] Y. Xiang, T. Schmidt, V. Narayanan, and D. Fox, "Posecnn: A convolutional neural network for 6d object pose estimation in cluttered scenes," *arXiv preprint arXiv:1711.00199*, 2017.
- [47] T. Hodaň, M. Sundermeyer, B. Drost, Y. Labbé, E. Brachmann, F. Michel, C. Rother, and J. Matas, "BOP challenge 2020 on 6D object localization," *European Conference on Computer Vision Workshops (ECCVW)*, 2020.
- [48] G. Quere, A. Hagengruber, M. Iskandar, S. Bustamante Gomez, D. Leidner, F. Stulp, and J. Vogel, "Shared control templates for assistive robotics," in *2020 IEEE International Conference on Robotics and Automation (ICRA)*, 2020.
- [49] M. Durner, W. Boerdijk, M. Sundermeyer, W. Friedl, Z.-C. Marton, and R. Triebel, "Unknown object segmentation from stereo images," *arXiv preprint arXiv:2103.06796*, 2021.
- [50] R. Girshick, I. Radosavovic, G. Gkioxari, P. Dollár, and K. He, "Detectron," <https://github.com/facebookresearch/detectron>, 2018.
- [51] T.-Y. Lin, M. Maire, S. Belongie, J. Hays, P. Perona, D. Ramanan, P. Dollár, and C. L. Zitnick, "Microsoft coco: Common objects in context," in *European conference on computer vision*. Springer, 2014, pp. 740–755.
- [52] M. Iskandar, G. Quere, A. Hagengruber, A. Dietrich, and J. Vogel, "Employing whole-body control in assistive robotics," in *2019 IEEE/RSJ International Conference on Intelligent Robots and Systems (IROS)*. IEEE, 2019, pp. 5643–5650.
- [53] S. Bustamante, G. Quere, K. Hagmann, X. Wu, P. Schmaus, J. Vogel, F. Stulp, and D. Leidner, "Toward seamless transitions between shared control and supervised autonomy in robotic assistance," *IEEE Robotics and Automation Letters*, vol. 6, no. 2, pp. 3833–3840, 2021.
- [54] A. Hagengruber and J. Vogel, "Functional tasks performed by people with severe muscular atrophy using an semg controlled robotic manipulator," in *2018 40th Annual International Conference of the IEEE Engineering in Medicine and Biology Society (EMBC)*. IEEE, 2018, pp. 1713–1718.